Support information

Synergy of mixed chromium species on NiFe layered double hydroxides for promoted alkaline water oxidation

Yongqiang Yang,[a] Jianlei Jing,[a] Zudong Shen,[a] Bo Li,[a] Mengze Ma,[a] Qihao Sha,[a] Wei Liu,[a] Xinlong Guo,[a] Shihang Li,[a] Zhichuan Li,[*b] Yun Kuang,[*c] Daojin Zhou[*a] and Xiaoming Sun[a]

a. State Key Laboratory of Chemical Resource Engineering, Beijing University of Chemical Technology, Beijing 100029, China.
b. Cnooc Energy Technology & Service Limited, Clean Energy Branch, Tianjin 300467, China.
c. Ocean Hydrogen Energy R&D Center, Research Institute of Tsinghua University in Shenzhen, Shenzhen 518057, China.
*E-mail: lizhch6@cnooc.com.cn; kuangy@tsinghua-sz.org; zhoudj@mail.buct.edu.cn

Experimental section

Synthesis of CO_3^{2-}-NiFeCr-LDH:

We prepared CO_3^{2-}-NiFeCr-LDH with varying molar ratios of Ni:Fe:Cr, including 6:2:1, 6:1:2, 6:1:1, and 4:1:1. Taking the preparation of CO_3^{2-}-NiFeCr(6:2:1)-LDH as an example, 3 mmol of $Ni(NO_3)_2{\cdot}6H_2O$, 1 mmol of $Fe(NO_3)_3{\cdot}9H_2O$, and 0.5 mmol of $Cr(NO_3)_3{\cdot}9H_2O$ were dissolved in 20 mL of deionized water to form solution A. Separately, 1 g of NaOH and 1 g of Na_2CO_3 were dissolved in 40 mL of deionized water to form solution B. Additionally, 2 g of Na_2CO_3 were dissolved in 50 mL of deionized water to form solution C. Under continuous stirring, solutions A and B were added dropwise into solution C while maintaining the pH at 10 throughout the process. The resulting turbid suspension was centrifuged, washed three times with deionized water, and freeze-dried under vacuum for 12 hours.

Synthesis of CrO_4^{2-}-NiFeCr-LDH:

We prepared CrO_4^{2-}-NiFeCr-LDH with varying molar ratios of Ni:Fe:Cr, including 6:2:1, 6:2:0. Taking the preparation of CrO_4^{2-}-NiFeCr(6:2:1)-LDH as an example, 3 mmol of $Ni(NO_3)_2{\cdot}6H_2O$, 1 mmol of $Fe(NO_3)_3{\cdot}9H_2O$, and 0.5 mmol of $Cr(NO_3)_3{\cdot}9H_2O$ were dissolved in 20 mL of deionized water to form solution A. Separately, 1 g of NaOH and 1 g of K_2CrO_4 were dissolved in 40 mL of deionized water to form solution B. Additionally, 2 g of K_2CrO_4 were dissolved in 50 mL of deionized water to form solution C. Under continuous stirring, solutions A and B were added dropwise into solution C while maintaining the pH at 10 throughout the process. The resulting turbid suspension was centrifuged, washed three times with deionized water, and freeze-dried under vacuum for 12 hours.

Physical characterization

The SEM images were obtained using Zeiss SUPRA55, and the corresponding EDS mapping data were characterized using an energy-dispersive spectrometer (Oxford). The XRD patterns were recorded on a Bruker D8A25 diffractometer, and the XPS spectra were acquired using a Shimadzu Axis Supra instrument. FT-IR spectra were measured on a Thermo Fisher Nicolet 6700

spectrometer, and ICP data were obtained using a Thermo Fisher ICAP-6300 instrument. Raman spectra were collected using LabRAM Aramis spectrometer.

Electrochemical measurement

The OER performance of the samples was evaluated using a three-electrode system. A platinum plate (1 × 1 cm^2) served as the counter electrode, and a Hg/HgO electrode was used as the reference electrode. The working electrode was prepared as follows: 5 mg of the sample was dispersed in 990 μL of ethanol, and 10 μL of 5% Nafion solution was added as a binder to form an ink. The ink was evenly drop-cast onto a nickel foam substrate and dried to obtain the working electrode. The three-electrode tests were conducted using an electrochemical workstation(DH7003 Donghua). For stability tests, a two-electrode system was employed, with the working electrode prepared using the same method as described above and a platinum plate (1 × 1 cm^2) serving as the counter electrode. The chronopotentiometry tests were conducting on CT2001A LANHE.

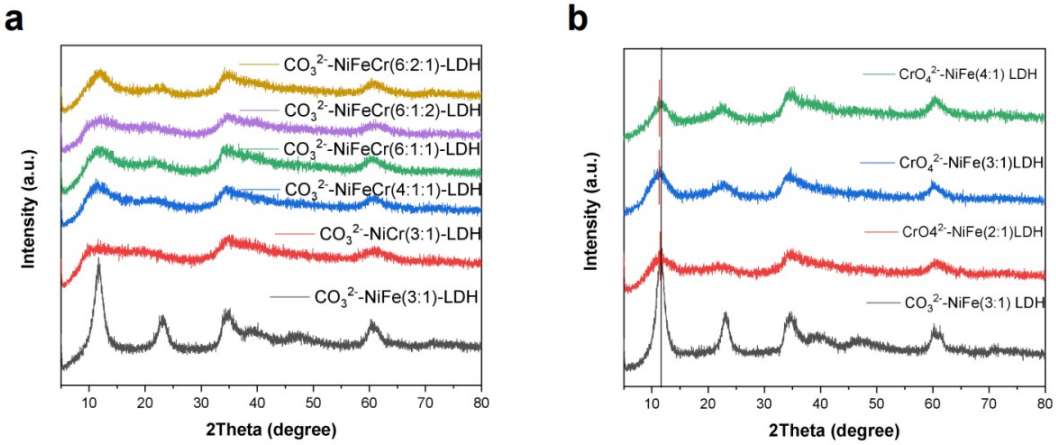

Figure S1. XRD patterns of (a) CO_3^{2-} intercalated NiFeCr-LDHs. (b)CrO_4^{2-} intercalated NiFe-LDH

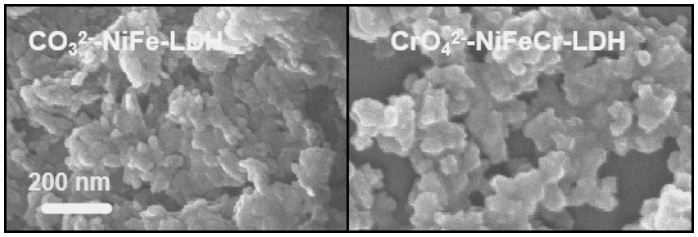

Figure S2. SEM images of CO_3^{2-}-NiFe-LDHs and CrO_4^{2-}-NiFeCr-LDHs.

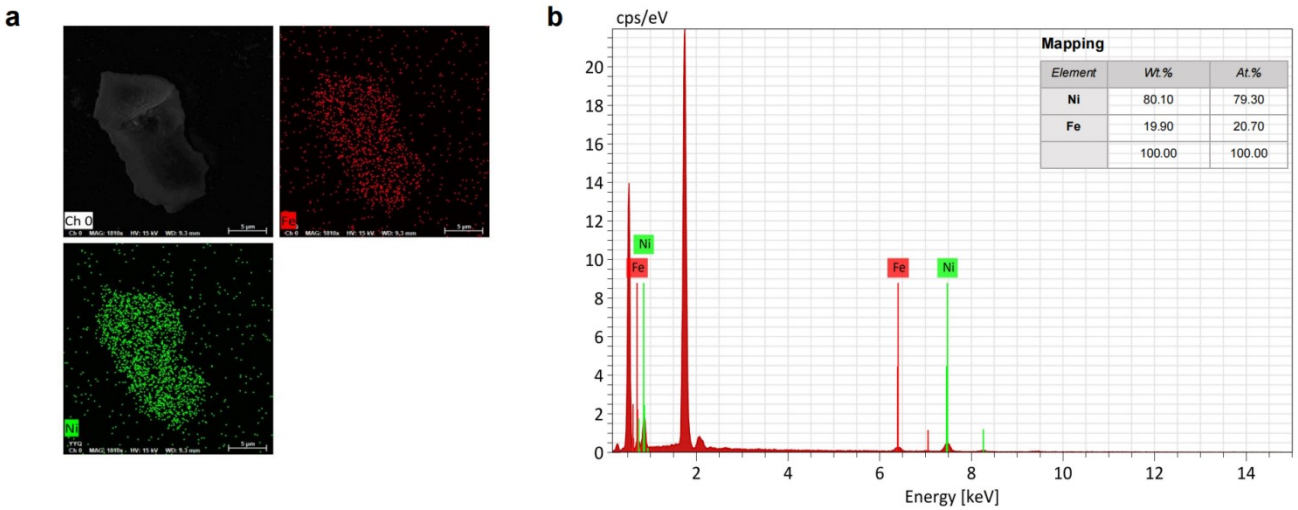

Figure S3. (a) EDS-mapping images of CO_3^{2-}-NiFe-LDH. (b) EDS spectra of CO_3^{2-}-NiFe-LDH and ratio of elements.

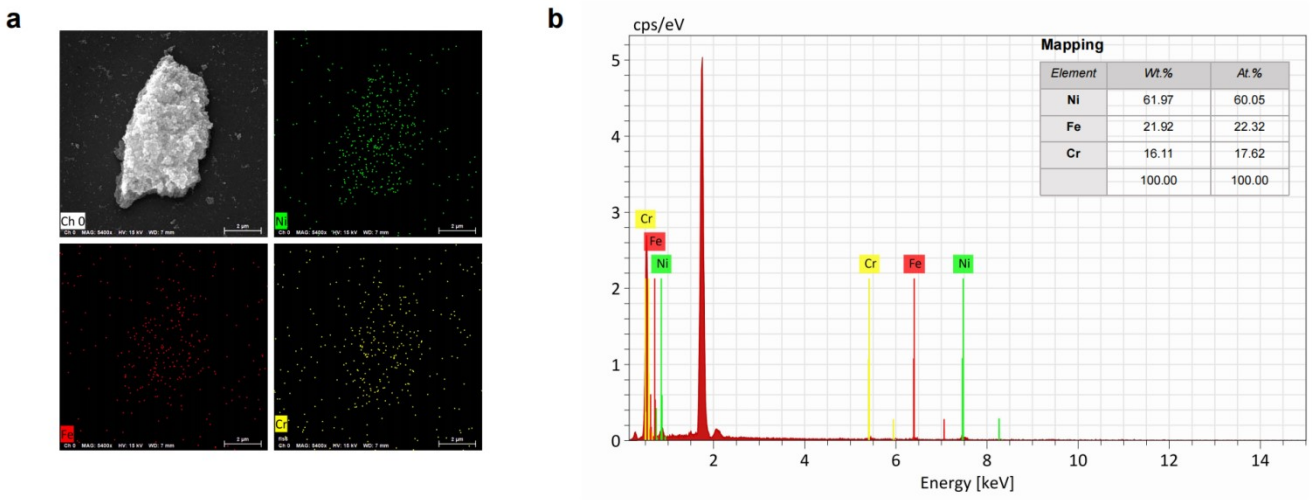

Figure S4. (a) EDS-mapping images of CrO_4^{2-}-NiFeCr-LDH. (b) EDS spectra of CrO_4^{2-}-NiFeCr-LDH and ratio of elements.

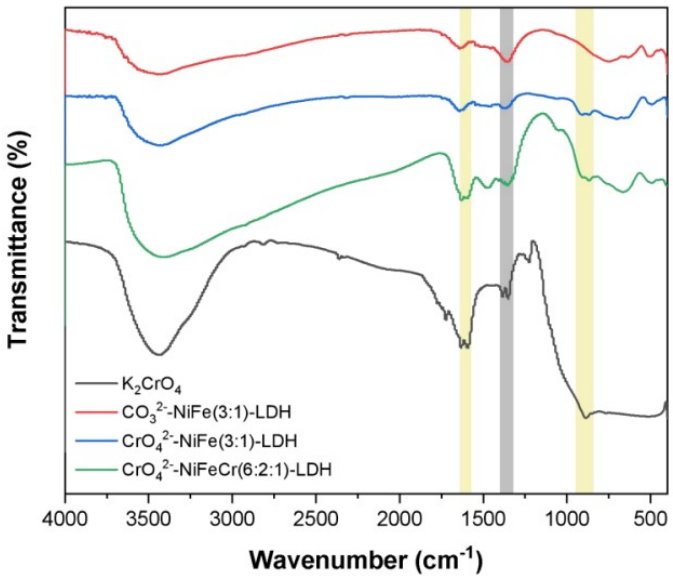

Figure S5. infrared spectra of K_2CrO_4 and LDHs.

Figure S6. XPS spectra of Cr 2P of LDHs.

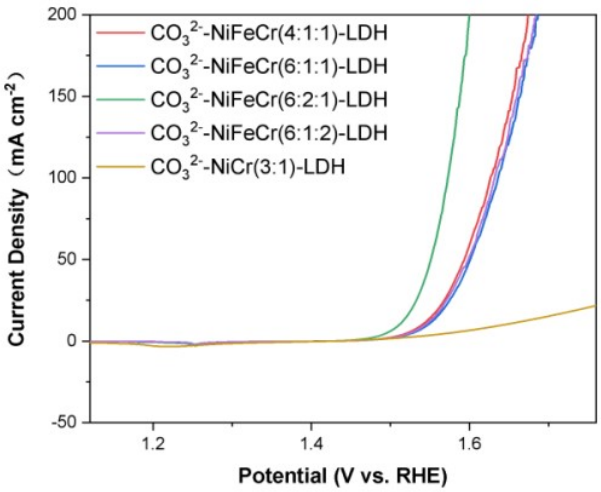

Figure S7. LSV curve of different Ni Fe Cr ratio LDH intercalated with CO_3^{2-}.

Figure S8. LSV curve of different Ni Fe ratio LDH intercalated with CrO_4^{2-}.

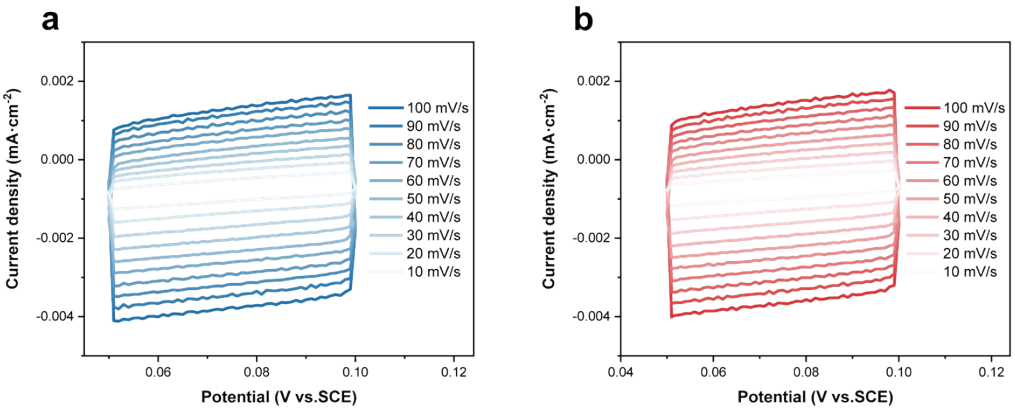

Figure S9. ECSA measurements of (a) CO_3^{2-}-NiFe-LDH, (b) CrO_4^{2-}-NiFeCr-LDH.

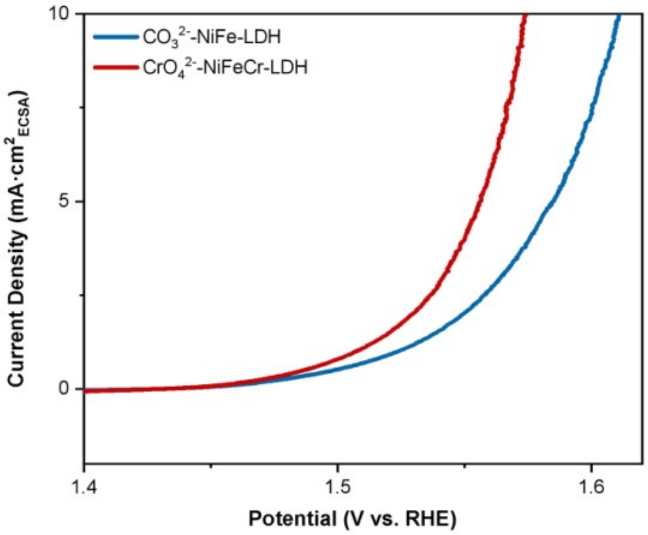

Figure S10. ECSA normalized LSV curve.

Figure S11. Nyquist plots tested at 0.4 V vs. reference electrode.

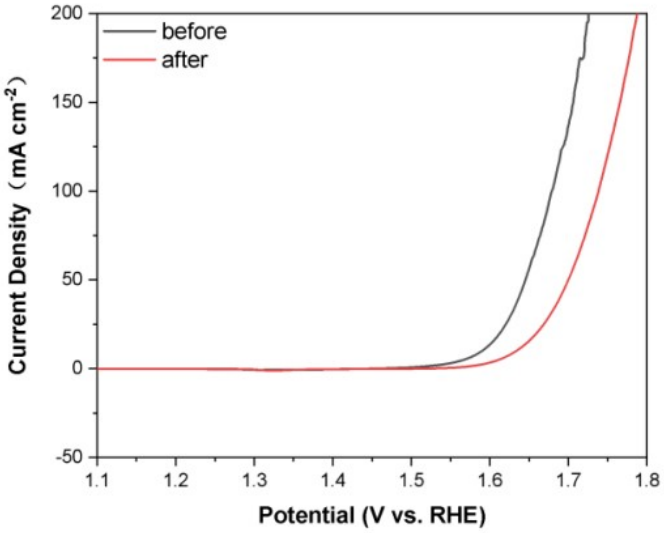

Figure S12. LSV curves of CO_3^{2-}-NiFeCr-LDH before and after stability test.

Figure S13. (a) LSV curves of CrO_4^{2-}-NiFeCr-LDH after stability test for different CrO_4^{2-} concentrations. (b) LSV curves of CrO_4^{2-}-NiFeCr-LDH before and after stability test in 0.5 mM CrO42-. (c) LSV curves of CrO42--NiFeCr-LDH before and after stability test in 1 mM CrO_4^{2-}. (d) LSV curves of CrO_4^{2-}-NiFeCr-LDH before and after stability test in 2 mM CrO_4^{2-}.

Figure S14. SEM images of CrO_4^{2-}-NiFeCr-LDH after stability test.

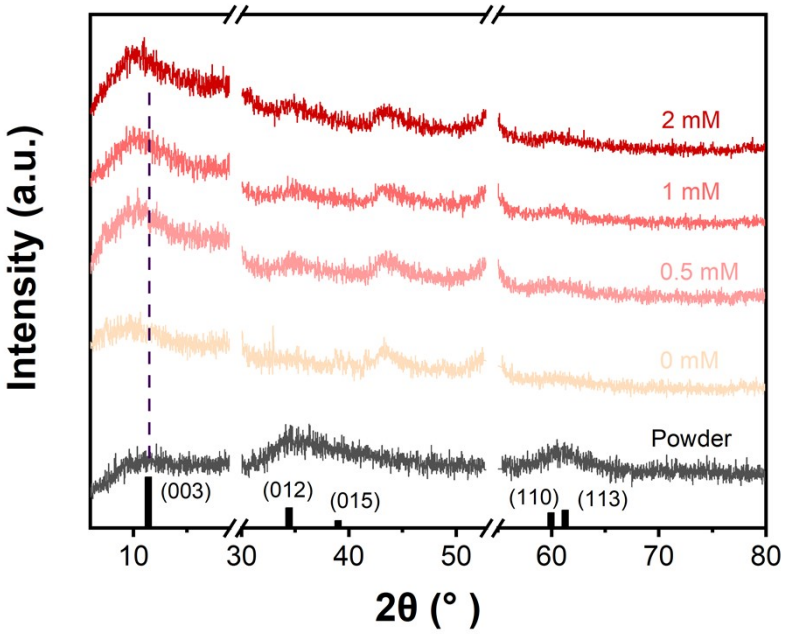

Figure S15. XRD patterns of CrO_4^{2-}-NiFeCr-LDH after stability test.

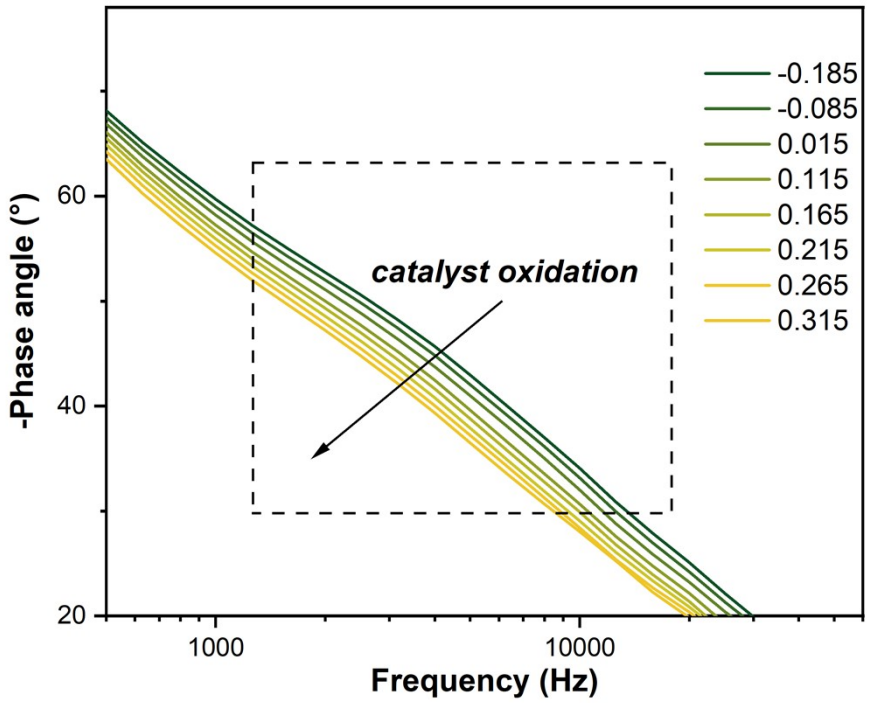

Figure S16. magnified operado bode plots of CrO_4^{2-}-NiFeCr-LDH.

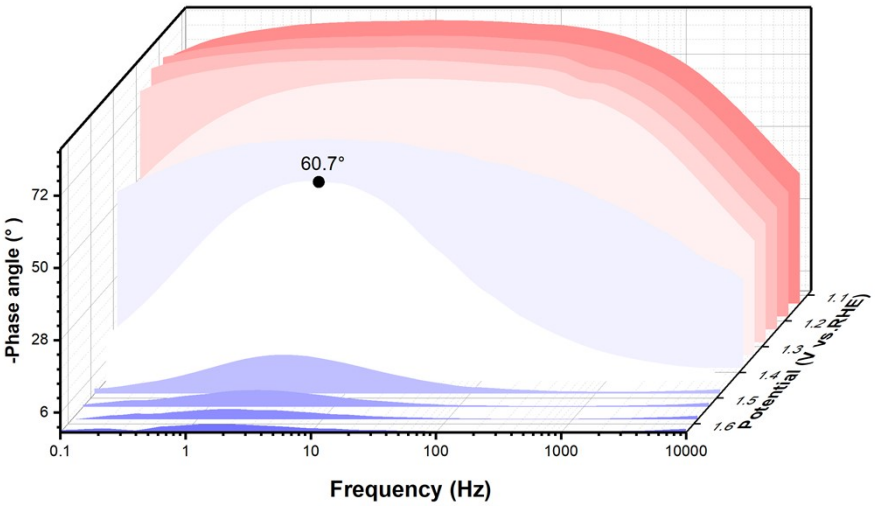

Figure S17. Operado bode plots of CrO_4^{2-}-NiFeCr-LDHs in 2 mM CrO_4^{2-}.

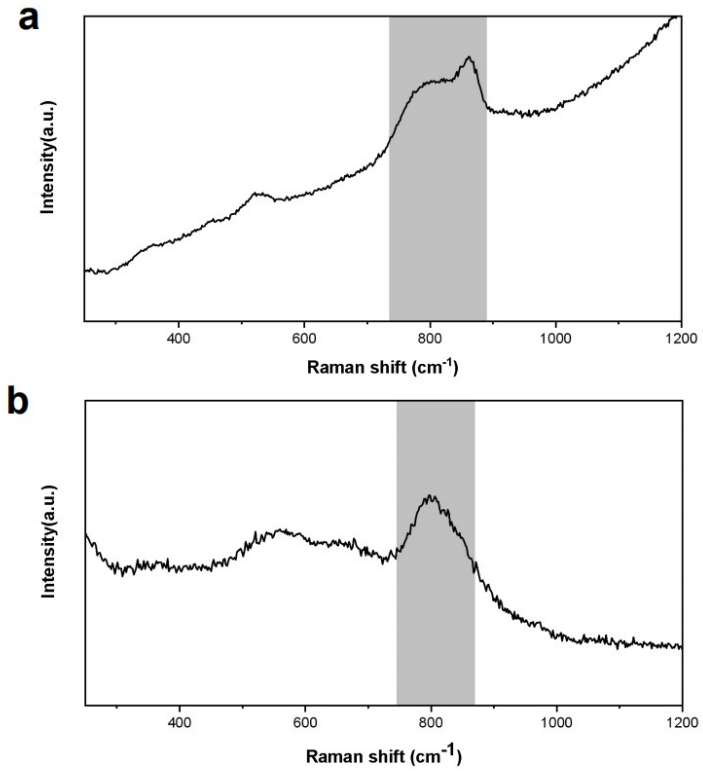

Figure S18. raman spectra of (a) CrO_4^{2-}-NiFe-LDH, (b) CO_3^{2-}-NiFeCr-LDH.

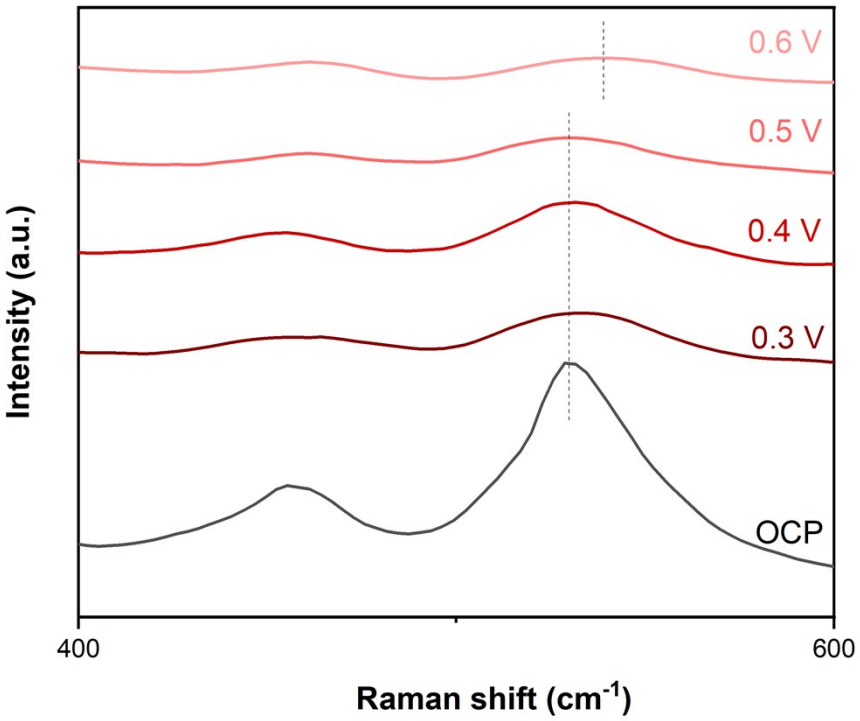

Figure S19. magnified in-situ raman spectra of CrO_4^{2-}-NiFeCr-LDH.

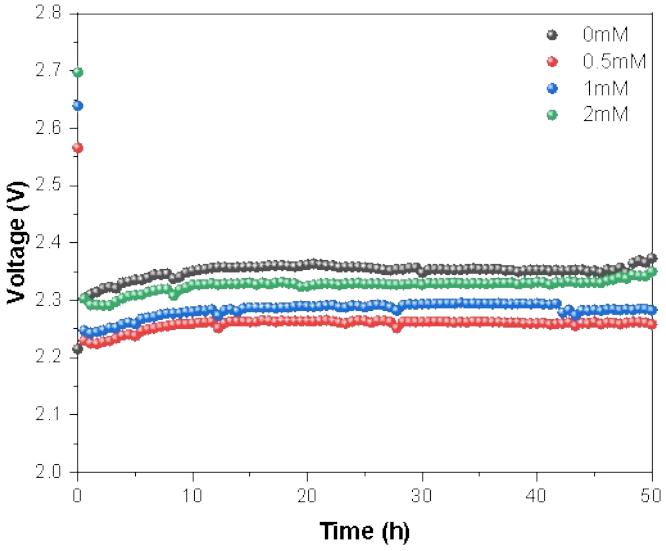

Figure S20. 50h OER stability test of CrO_4^{2-}-NiFeCr-LDH in chromate electrolyte with different concentrations at a current density of 400 mA·cm^{-2} at 80℃.

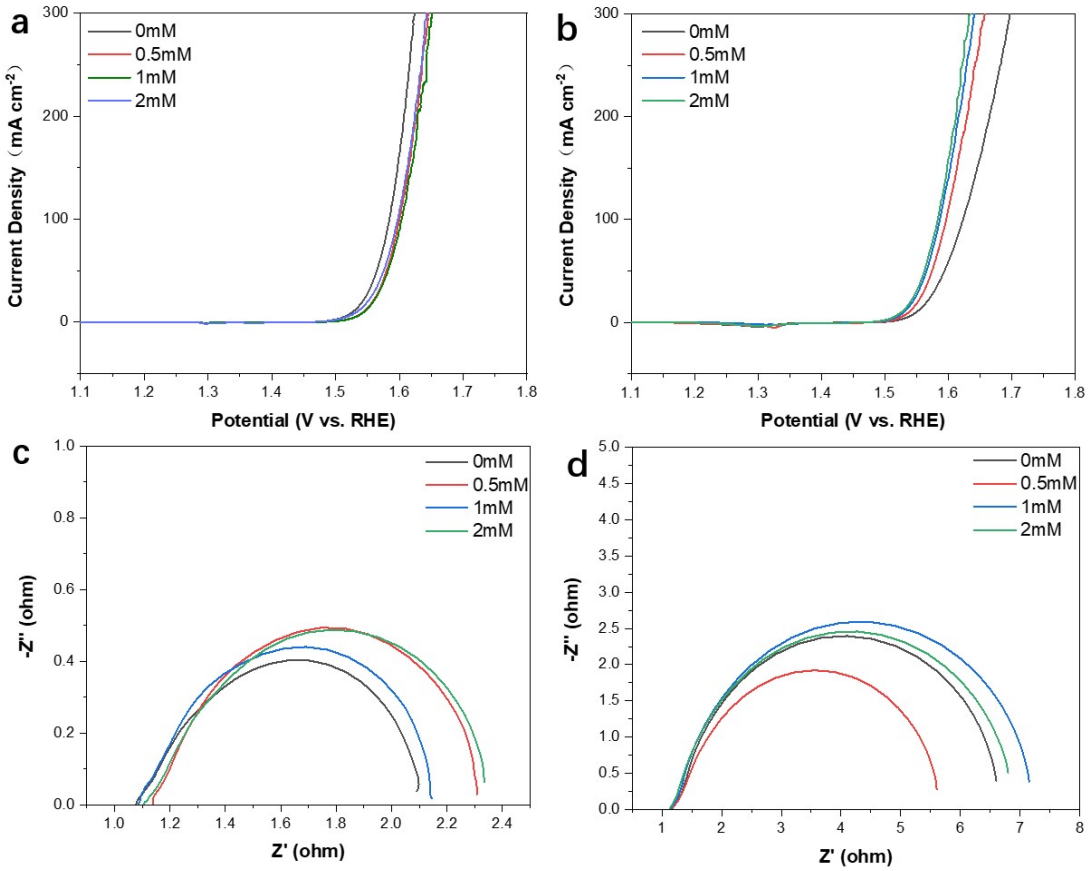

Figure S21. CrO_4^{2-}-NiFeCr-LDH in different concentrations of CrO_4^{2-} electrolyte at 80 ℃ (a) polarization curves before stability test; (b) Polarization curves after stability test; (c) EIS spectrum before stability test; (d) EIS spectrum after stability test.

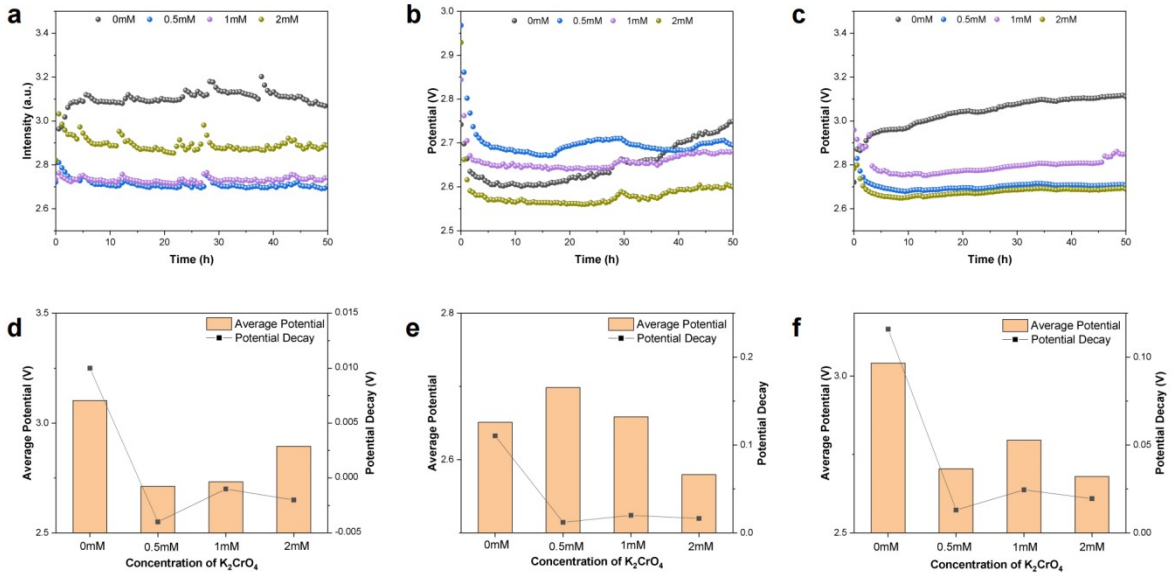

Figure S22. Chronopotentiometric curves of different electrocatalyst samples for stability test (a) CO_3^{2-}-NiFeCr-LDH; (b) CrO_4^{2-}-NiFe-LDH; (c) CO_3^{2-}-NiFe-LDH; Average voltage and voltage variation of samples of different electrocatalysts (d) CO_3^{2-}-NiFeCr-LDH; (e) CrO_4^{2-}-NiFe-LDH; (f） CO_3^{2-}-NiFe-LDH.

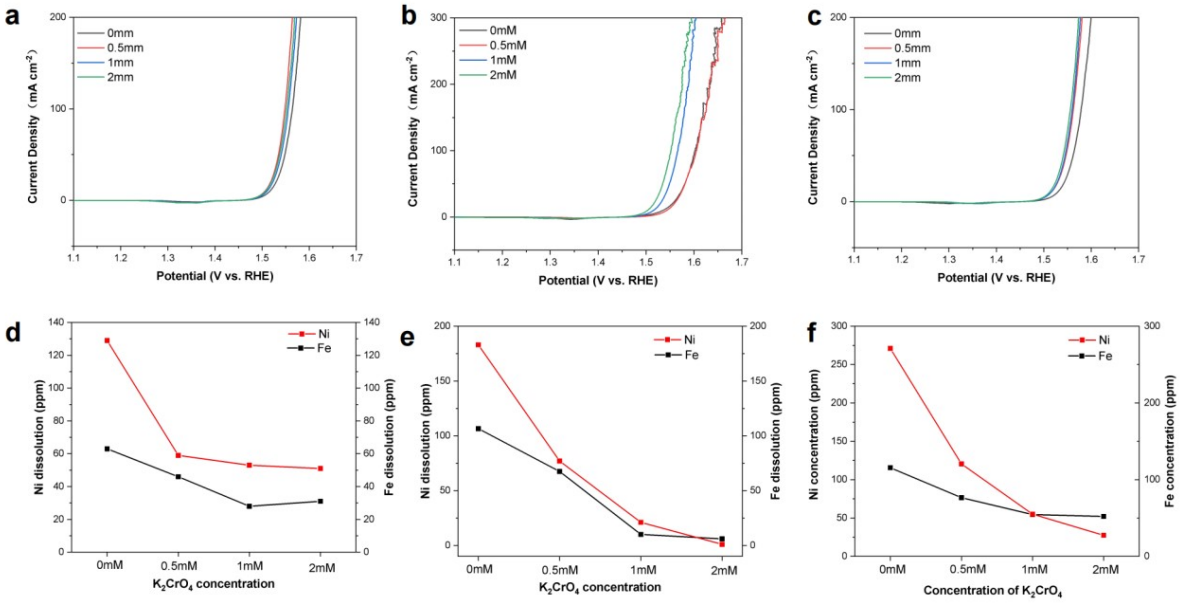

Figure S23. LSV curves after stability test of different electrocatalyst samples (a) CO_3^{2-}-NiFeCr-LDH, (b) CrO_4^{2-}-NiFe-LDH, (c) CO_3^{2-}-NiFe-LDH, dissolution amount of Ni and Fe in electrolyte, (d) CO_3^{2-}-NiFeCr-LDH, (e) CrO_4^{2-}-NiFe-LDH, (f) CO_3^{2-}-NiFe-LDH.

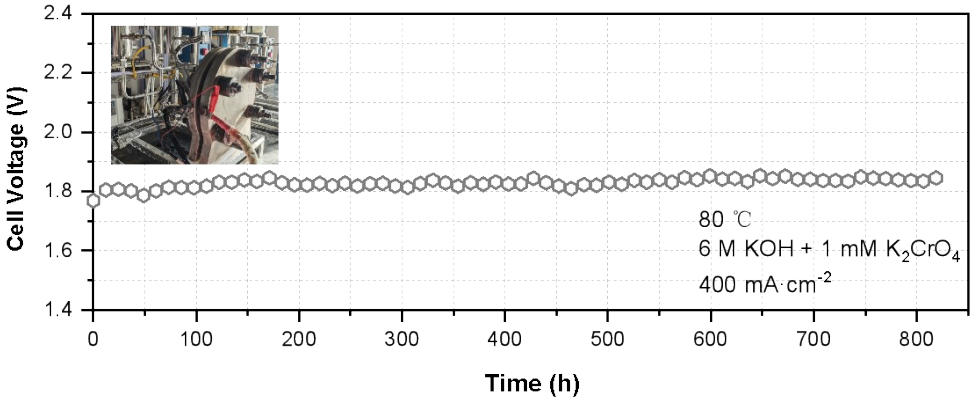

Figure S24. Chronopotentiometric curves of CrO_4^{2-}-NiFe-LDH based AWE at 400 mA·cm^{-2}.